Instantaneous Frequency Estimation in Unbalanced Systems Using Affine Differential Geometry

Ali Alshawabkeh, Georgios Tzounas, *Member, IEEE*, and Federico Milano, *Fellow, IEEE*

***Abstract*—The paper discusses the relationships between electrical quantities, namely voltages and frequency, and affine differential geometry ones, namely affine arc length and curvature. Moreover, it establishes a link between frequency and time derivatives of voltage, through the utilization of affine differential geometry invariants. Based on this link, a new instantaneous frequency estimation formula is proposed, which is particularly suited for unbalanced systems. An application of the proposed formula to single-phase systems is also provided. Several numerical examples based on balanced, unbalanced, as well as single-phase systems illustrate the findings of the paper.**

***Index Terms*—Frequency estimation, affine differential geometry, instantaneous frequency, unbalanced systems, curvature, phase-locked loop (PLL).**

I. Introduction

A. Motivation

On-line frequency estimation in electric power systems is known to be a complex problem, especially in conditions characterized by the presence of harmonics and imbalances of amplitude or phase angle within the measured signals. Aiming in particular to tackle the complexities posed by unbalanced systems, this paper introduces a technique for on-line frequency estimation, based on the principles of affine differential geometry.

B. Literature Review

The problem of frequency estimation has been studied for many years and several solution approaches have been reported in the literature, e.g. see [1]–[10]. These approaches rely on a variety of methods, including phase-locked loops (PLLs) [1], [2], discrete Fourier transform [3], [4], Kalman filtering [5], [6], least-squares [7], [8], adaptive notch filters [9], [10], etc.

For grid synchronization and control applications in particular, PLLs are a popular solution due their performance characteristics and straightforward structure and practical implementation. Three-phase PLLs, for example, are widely utilized to provide on-line phase and frequency estimations in grid-connected power converters. With this regard, a conventional PLL configuration in three-phase system applications is the synchronous reference frame (SRF) PLL, which relies on transforming input voltages to the dq synchronous reference frame and on regulating the frame's angular position so that either the d- or q-axis component is zero. The analogous of SRF-PLL for single-phase systems is the quadrature signal generation (QSG)-based PLL. Given a single-phase voltage signal, a QSG-PLL defines a second dimension through a fictitious quadrature signal, required to enable the application of the Park transform (and thus the formulation of dq-axis voltage components). The simplest approach to do that is using a *transport delay* of $T/4$, where T is the period of the fundamental frequency, e.g. see [11].

Other approaches are based on the inverse Park transform [12], the Hilbert transform [13], and on second-order generalized integrators [14]. Although they provide robust frequency estimations under balanced conditions, they are also known to perform poorly for unbalanced systems, wherein they often result in estimations with sinusoidal ripple errors [15]–[19]. Reducing the bandwidth helps mitigate this issue and refine accuracy, but also compromises dynamic performance [20]. In this regard, careful tuning of PLL parameters is essential to achieve good trade-offs between dynamic performance and estimation accuracy. Efforts to improve the performance of PLLs under unbalanced conditions include, among other studies, [1], [17], [21], [22].

PLLs belong to the broad family of time-domain methods. In this paper we also focus on time-domain methods but approach the problem of frequency estimation from an unconventional perspective, that is based on the theory of differential geometry. The starting assumption is that any voltage vector can be perceived as the velocity of a point on a space curve and, as such, be analyzed using differential geometrical invariants. In our recent work on the topic, we described the definition of these curves in a Euclidean space and, by applying the Frenet–Serret formulas, we derived a correspondence between curvature and instantaneous electrical frequency [23]–[26]. Despite providing accurate frequency estimations for balanced systems, the curvature obtained in these works is time-varying in stationary unbalanced operating conditions, a result that clearly does not align well with the notion of angular frequency of stationary ac signals.

In this paper, we aim at solving this issue through an alternative theory of differential geometry of curves, namely through *affine differential geometry*. This theory has found applications in various areas, such as control of mechanical systems [27], computer vision [28], and motion identification [29]. But there has been, to the best of our knowledge, no application to power system analysis or frequency estimation.

A. Alshawabkeh, G. Tzounas and F. Milano are with School of Electrical and Electronic Engineering, University College Dublin, Dublin, D04V1W8, Ireland. E-mails: ali.alshawabkeh@ucdconnect.ie, {georgios.tzounas, federico.milano}@ucd.ie

This work is supported by the Sustainable Energy Authority of Ireland (SEAI) by funding A. Alshawabkeh and F. Milano under project FRESLIPS, Grant No. RDD/00681.

C. Contributions

The specific contributions of the paper are as follows.

- A derivation of the expressions for the affine arc length and affine curvature in terms of the voltage of an ac system.
- An approximated yet accurate formula of the instantaneous angular frequency of a three-phase voltage as a function of affine geometrical invariants.
- A demonstration of the effectiveness of the proposed formula to serve as an instantaneous frequency estimation technique for unbalanced three-phase systems, as well as for single-phase systems.

The last two points are fully supported through a variety of examples, which are provided in the case study section. The examples show, in particular, that the proposed expression yields a more precise estimation of the instantaneous frequency in unbalanced systems, compared to PLLs and the Frenet-frame based method from [23].

D. Paper Organization

The remainder of the paper is organized as follows. Section II provides an overview of basic concepts from affine geometry. These concepts are essential for the derivation of the theoretical results of the paper presented in Section III. Section IV tests the proposed approach through analytical examples, as well as through a case study based on a fully-fledged EMT model of the IEEE 39-bus system. Finally, Section V draws relevant conclusions.

II. Outlines of Affine Differential Geometry

This section provides a brief overview of affine quantities that are relevant for the derivation of the instantaneous frequency formula for ac systems presented in Section III. The interested reader can find a comprehensive presentation of the theory of affine differential geometry in [30].

Affine geometry can be defined as a Euclidean geometry without measuring distances or angles. In other words, it is a Euclidean geometry whose metric structure has been removed [29]. For the affine plane, a pair of non-collinear vectors determines a parallelogram whose area is given by the determinant of the two-by-two matrix formed by these vectors.

Let us consider a smooth parametric curve in the plane:

$$\boldsymbol{x}(t) = x_1(t)\,\boldsymbol{e}_1 + x_2(t)\,\boldsymbol{e}_2\,, \tag{1}$$

where $x_1(t), x_2(t) : \mathbb{R} \mapsto \mathbb{R}$ are smooth and $\boldsymbol{e}_1$ and $\boldsymbol{e}_2$ form an orthogonal basis of the plane. Let us also assume that the curve $\boldsymbol{x}$ does not have inflection points, that is, the magnitude of the bracket operator

$$[\dot{\boldsymbol{x}}(t), \ddot{\boldsymbol{x}}(t)] \neq 0, \quad \forall t\,, \tag{2}$$

never vanishes. In (2), $\dot{\boldsymbol{x}} = d\boldsymbol{x}/dt$ and $\ddot{\boldsymbol{x}} = d^2\boldsymbol{x}/dt^2$, and the bracket operator of two vectors, say $[\boldsymbol{a}, \boldsymbol{b}]$, with $\boldsymbol{a}, \boldsymbol{b} \in \mathbb{R}^2$, is defined as:

$$[\boldsymbol{a}, \boldsymbol{b}] = \det \begin{vmatrix} a_1 & b_1 \\ a_2 & b_2 \end{vmatrix} = a_1 b_2 - b_1 a_2\,, \tag{3}$$

The *affine arc length* or *equi-affine arc length*, indicated with σ, is defined as:

$$\sigma(t) = \int_{t_0}^{t} [\dot{\boldsymbol{x}}(t), \ddot{\boldsymbol{x}}(t)]^{1/3} dt\,, \tag{4}$$

or, equivalently:

$$\dot{\sigma}(t) = \frac{d\sigma(t)}{dt} = [\dot{\boldsymbol{x}}(t), \ddot{\boldsymbol{x}}(t)]^{1/3}\,. \tag{5}$$

A curve $\boldsymbol{x}$ is said to be parameterized with σ if, for all σ, it satisfies the condition:

$$[\boldsymbol{x}'(\sigma), \boldsymbol{x}''(\sigma)] = 1\,, \tag{6}$$

where $\boldsymbol{x}' = d\boldsymbol{x}/d\sigma$ is the *affine tangent* and $\boldsymbol{x}'' = d^2\boldsymbol{x}/d\sigma^2$ is the *affine normal*. Applying the chain rule, $\boldsymbol{x}'$ becomes:

$$\boldsymbol{x}'(\sigma(t)) = \frac{d\boldsymbol{x}}{d\sigma} = \frac{d\boldsymbol{x}}{dt}\frac{dt}{d\sigma} = \frac{\dot{\boldsymbol{x}}(t)}{[\dot{\boldsymbol{x}}(t), \ddot{\boldsymbol{x}}(t)]^{1/3}}\,, \tag{7}$$

and, differentiating (6) with respect to σ, one obtains:

$$[\boldsymbol{x}'(\sigma), \boldsymbol{x}'''(\sigma)] = 0\,. \tag{8}$$

This result implies that $\boldsymbol{x}'$ and $\boldsymbol{x}'''$ are linearly independent, leading to the relationship:

$$\boldsymbol{x}'''(\sigma) = -\kappa_a(\sigma)\,\boldsymbol{x}'(\sigma)\,, \tag{9}$$

where κ_a is the *affine curvature* or *equi-affine curvature* of the curve $\boldsymbol{x}$ and is defined as:

$$\kappa_a(\sigma) = [\boldsymbol{x}''(\sigma), \boldsymbol{x}'''(\sigma)]\,. \tag{10}$$

The affine curvature is represented by the area of the parallelogram formed by the vectors $\boldsymbol{x}''$ and $\boldsymbol{x}'''$.

It is relevant for the following discussion on the estimation of the instantaneous frequency to note that for non-singular conic sections, κ_a is constant, as follows [30], [31]:

- for $\kappa_a = 0$, the curve is a parabola;
- for $\kappa_a > 0$, the curve is an ellipse;
- for $\kappa_a < 0$, the curve is an hyperbola.

In the next section, we consider the specific case of the ellipse, that is $\kappa_a > 0$.

III. Voltage in the Affine Plane

We adopt the assumption made in [25], that is, the magnetic flux $\boldsymbol{\varphi}$ is the *position* of a point on a space curve in generalized coordinates and, from Faraday's law, the *speed* of such a point is the voltage, as follows:

$$\boldsymbol{\varphi}(t) \equiv -\boldsymbol{x}(t) \quad \Rightarrow \quad \boldsymbol{v}(t) = -\dot{\boldsymbol{\varphi}}(t) \equiv \dot{\boldsymbol{x}}(t)\,. \tag{11}$$

Reference [23] shows that one can express electrical quantities such as voltage and current in terms of the coordinates of the Frenet frame and of geometric invariants such as arc length, curvature and torsion [23]. In the same vein, but using the definitions of coordinates, arc length and curvature given by affine differential geometry, this section derives a new formula for the instantaneous frequency of electrical quantities. In the remainder of this section, we discuss exclusively voltages, but the same procedure and results can be obtained using currents. We consider two scenarios, namely unbalanced three-phase systems; and single-phase systems.

A. Three-Phase Unbalanced Voltages

Let's assume that the phases abc of a three-phase voltage $\boldsymbol{v}(t)$ constitute a set of orthogonal coordinates:

$$\boldsymbol{v}(t) = v_{\mathrm{a}}(t)\,\boldsymbol{e}_{\mathrm{a}} + v_{\mathrm{b}}(t)\,\boldsymbol{e}_{\mathrm{b}} + v_{\mathrm{c}}(t)\,\boldsymbol{e}_{\mathrm{c}}\,. \tag{12}$$

In order to employ the theory described in the previous section, which applies to curves in two dimensions, we first need to transform the voltage $\boldsymbol{v}(t)$ into the following shape:

$$\boldsymbol{v}(t) = v_1(t)\,\boldsymbol{e}_1 + v_2(t)\,\boldsymbol{e}_2\,. \tag{13}$$

This is conveniently achieved by applying the Clarke transform to (12) and taking the α and β components, as follows:

$$\begin{bmatrix} v_\alpha(t) \\ v_\beta(t) \end{bmatrix} = \frac{2}{3}\begin{bmatrix} 1 & -\frac{1}{2} & -\frac{1}{2} \\ 0 & \frac{\sqrt{3}}{2} & -\frac{\sqrt{3}}{2} \end{bmatrix}\begin{bmatrix} v_{\mathrm{a}}(t) \\ v_{\mathrm{b}}(t) \\ v_{\mathrm{c}}(t) \end{bmatrix}. \tag{14}$$

Thus, the components of the voltage in (13) are:

$$v_1(t) = v_\alpha(t)\,, \qquad v_2(t) = v_\beta(t)\,. \tag{15}$$

1) Stationary Sinusoidal Voltages: We discuss in this section a "base case" scenario for which the theory of affine differential geometry allows obtaining the exact value of the frequency of the voltage. This is the case of an unbalanced stationary sinusoidal (i.e., without harmonics) three-phase voltage. As discussed above, since we apply the Clarke transform, the components of the voltage vector in (13) are:

$$v_1(t) = V_1\cos\theta(t)\,, \qquad v_2(t) = V_2\sin\theta(t)\,, \tag{16}$$

where V_1 and V_2 are constant with $V_1 \neq V_2$, and:

$$\theta(t) = \omega_o t + \theta_o\,, \tag{17}$$

where ω_o is the fundamental synchronous reference frequency of the system and θ_o is constant and depends on the chosen phase angle reference of the system.

With the equivalence given in (11), the time derivative of the affine arc length $\dot\sigma$ in (5) can be written as:

$$\dot\sigma = [\boldsymbol{v}(t), \dot{\boldsymbol{v}}(t)]^{1/3} = (\omega_o V_1 V_2)^{1/3}\,. \tag{18}$$

Note that while $\boldsymbol{v}$ and $\dot{\boldsymbol{v}}$ depend on time, $\dot\sigma$ does not. Then, imposing that the components of the voltage are as those given in (16), one obtains:

$$\boldsymbol{x}'(t) = \frac{\boldsymbol{v}(t)}{\dot\sigma}\,, \quad \boldsymbol{x}''(t) = \frac{\dot{\boldsymbol{v}}(t)}{\dot\sigma^2}\,, \quad \boldsymbol{x}'''(t) = \frac{\ddot{\boldsymbol{v}}(t)}{\dot\sigma^3}\,, \tag{19}$$

where

$$\begin{aligned} \boldsymbol{v}(t) &= V_1\cos\theta(t)\,\boldsymbol{e}_1 + V_2\sin\theta(t)\,\boldsymbol{e}_2\,, \\ \dot{\boldsymbol{v}}(t) &= -\omega_o V_1\sin\theta(t)\,\boldsymbol{e}_1 + \omega_o V_2\cos\theta(t)\,\boldsymbol{e}_2\,, \\ \ddot{\boldsymbol{v}}(t) &= -\omega_o^2 V_1\cos\theta(t)\,\boldsymbol{e}_1 - \omega_o^2 V_2\sin\theta(t)\,\boldsymbol{e}_2\,. \end{aligned} \tag{20}$$

Then, using (10), (18) and (19), the expression of the affine curvature κ_a becomes:

$$\kappa_a = \frac{1}{\dot\sigma^5}[\dot{\boldsymbol{v}}(t), \ddot{\boldsymbol{v}}(t)] = \frac{\omega_o^3 V_1 V_2}{\dot\sigma^5}\,, \tag{21}$$

where κ_a is constant, which is as expected since (16) describes an ellipse in the plane (v_1, v_2). Merging (18) and (21) we obtain:

$$\omega_o = \sqrt{\kappa_a}\,\dot\sigma = \sqrt{\frac{[\dot{\boldsymbol{v}}(t), \ddot{\boldsymbol{v}}(t)]}{[\boldsymbol{v}(t), \dot{\boldsymbol{v}}(t)]}}\,. \tag{22}$$

Equation (22) indicates that, in order to calculate the angular frequency of the voltage in unbalanced conditions, it suffices to measure $\boldsymbol{v}$ and estimate its first and second time derivatives.

2) Transient Voltages: Section III-A1 considers an ideal scenario for which the magnitude and the angular frequency of a three-phase voltage are constant. This scenario leads to a compact and elegant analytical result. However, such scenario is hardly found in practice, wherein the presence of noise, harmonics, and transient conditions prevents obtaining a general explicit expression for the instantaneous frequency.

Under certain conditions, however, it is still possible to utilize the results of Section III-A1 for a voltage of time-varying angular frequency and/or magnitudes of v_1 and v_2. Consider a time-varying voltage vector:

$$\boldsymbol{v}(t) = V_1(t)\cos\vartheta(t)\,\boldsymbol{e}_1 + V_2(t)\sin\vartheta(t)\,\boldsymbol{e}_2\,, \tag{23}$$

where $\vartheta(t) = \omega_o t + \phi(t)$. The conditions so that (22) holds for a voltage $\boldsymbol{v}(t)$ in the form of (23) are:

$$\frac{d^h}{dt^h}\phi(t) \ll \omega_o^h\,, \quad h = 1, 2\,, \tag{24}$$

$$\frac{d^h}{dt^h}\frac{V_i(t)}{\langle V_i\rangle} \ll \omega_o^h\,, \quad i, h = 1, 2\,, \tag{25}$$

where $\langle\cdot\rangle$ denotes the average value. Condition (24) for $h = 1$ indicates that the variation of the instantaneous frequency of the voltage is close to the synchronous reference angular frequency of the system; for $h = 2$, (24) imposes a boundary to the rate of change of frequency (RoCoF); and conditions (25) impose that the variations of the *radial frequency* (see definition in [25]) are small compared to the fundamental frequency of the grid. All these assumptions are generally well satisfied in power systems.

Conditions (24) and (25) are sufficient for (22) to hold at least as a first order approximation. In fact, the first time derivative of the voltage vector in (23) is:

$$\dot{\boldsymbol{v}} = (\dot V_1\cos\vartheta - \dot\vartheta V_1\sin\vartheta)\,\boldsymbol{e}_1 + (\dot V_2\sin\vartheta + \dot\vartheta V_2\cos\vartheta)\,\boldsymbol{e}_2\,,$$

and the second time derivative is:

$$\begin{aligned} \ddot{\boldsymbol{v}} = &-\left(\ddot\vartheta V_1\sin\vartheta + \dot\vartheta^2 V_1\cos\vartheta + \dot\vartheta\dot V_1\sin\vartheta - \ddot V_1\cos\vartheta\right)\boldsymbol{e}_1 \\ &+\left(\ddot\vartheta V_2\cos\vartheta + \dot\vartheta^2 V_2\sin\vartheta + \dot\vartheta\dot V_2\cos\vartheta - \ddot V_2\sin\vartheta\right)\boldsymbol{e}_2\,, \end{aligned}$$

where the dependency on time has been omitted for economy of notation.

It is straightforward to show that by applying (24) and (25), the voltage derivatives can be approximated with the second and third equations of (20) and, hence, the instantaneous frequency can be approximated using (22). In summary, (24) and (25) lead to the following approximated expression of the instantaneous frequency of a time-varying unbalanced voltage:

$$\dot\vartheta(t) \approx \boxed{\omega_a(t) = \sqrt{\frac{[\dot{\boldsymbol{v}}(t), \ddot{\boldsymbol{v}}(t)]}{[\boldsymbol{v}(t), \dot{\boldsymbol{v}}(t)]}}} \tag{26}$$

The expression of ω_a in (26) is the main result of this work. We test the accuracy of (26) through a variety of examples and a case study in Section IV.

B. Single-Phase Voltages

In this section we consider a single-phase voltage with instantaneous value $v(t)$. To apply the theory described in Section II, we first need to transform $v(t)$ into the shape of (13). To this aim, we construct the second dimension by employing the voltage derivative. That is:

$$v_1(t) = v(t)\,, \qquad v_2(t) = \dot{v}(t)\,. \tag{27}$$

Since the time derivative of sinusoidal signals gives a 90° rotation, using the time derivative is equivalent to defining a quadrature axis (see also discussion on quadrature signal generation in Section I).

1) Stationary Sinusoidal Voltages: The result obtained in the previous section can be easily extended to a stationary sinusoidal single-phase voltage using (27). Let the voltage be:

$$v(t) = V\cos\theta(t)\,, \tag{28}$$

where V is constant and θ is defined in (17). Then, from (27), the components of the voltage vector are:

$$v_1(t) = V\cos\theta(t)\,, \qquad v_2(t) = -\omega_o V\sin\theta(t)\,. \tag{29}$$

Substituting $V_1 = V$ and $V_2 = \omega_o V$ in (18) and (21), one obtains:

$$\dot{\sigma} = (\omega_o V)^{2/3}\,, \quad \kappa_a = \frac{\omega_o^4 V^2}{\dot{\sigma}^5}\,. \tag{30}$$

Apart from the fact that calculation of $\ddot{\boldsymbol{v}}(t)$ in this case requires the additional step of computing the third derivative of $v(t)$, equation (22) holds and allows estimating the angular frequency also for a single-phase voltage.

2) Transient Voltages: Consider a time-varying single-phase voltage:

$$v(t) = V(t)\cos\vartheta(t)\,, \tag{31}$$

where $\vartheta(t) = \omega_o t + \phi(t)$. The voltage vector is defined as:

$$\begin{aligned}\boldsymbol{v}(t) &= V(t)\cos\vartheta(t)\,\boldsymbol{e}_1 \\ &\quad + [\dot{V}(t)\cos\vartheta(t) - V(t)\dot{\vartheta}(t)\sin\vartheta(t)]\,\boldsymbol{e}_2\,.\end{aligned} \tag{32}$$

If one assumes:

$$\frac{d^h}{dt^h}\phi(t) \ll \omega_o^h\,, \quad h = 1,2,3\,, \tag{33}$$

$$\frac{d^h}{dt^h}\frac{V(t)}{\langle V_i\rangle} \ll \omega_o^h\,, \quad h = 1,2,3\,, \tag{34}$$

then (26) is also a good approximation of the instantaneous frequency of the time-varying single-phase voltage in (31).

IV. Case Studies

The examples discussed in this section are aimed at illustrating the accuracy of (26) for both unbalanced three- and single-phase voltages in various non-sinusoidal and non-stationary conditions. The proposed approach is compared with a conventional technique, namely the SRF-PLL, as well as with the Frenet frame-based method proposed in [23]. The first section of the study focuses on three-phase systems under various conditions. Both balanced and unbalanced cases are discussed. The IEEE 39-bus system is also utilized to illustrate the accuracy of the proposed method under transient unbalanced conditions. Finally, an example discussing the frequency estimation for a non-stationary single-phase voltage is presented.

In all figures shown in this section, ω_a represents the estimated angular frequency derived from the proposed approach, while ω_κ represents the estimated angular frequency obtained using the Frenet frame-based method from [23], as follows:

$$\omega_\kappa(t) = \frac{[\boldsymbol{v}(t), \dot{\boldsymbol{v}}(t)]}{|\boldsymbol{v}(t)|^2}\,. \tag{35}$$

The three-phase voltage trajectories are given in per unit (pu) with respect to a base of 12 kV, and ω_a and ω_κ are in pu with respect to $\omega_o = 100\pi$ rad/s. Finally, note that in all examples, (26) is calculated using a sampling of the voltage signal, transforming it through the Clarke transform and then evaluating numerically the time derivatives of the α and β components.

A. Three-Phase Voltage

Let us consider the three-phase voltage vector given in (12), which we repeat here for convenience:

$$\boldsymbol{v}(t) = v_{\rm a}(t)\,\boldsymbol{e}_{\rm a} + v_{\rm b}(t)\,\boldsymbol{e}_{\rm b} + v_{\rm c}(t)\,\boldsymbol{e}_{\rm c}\,, \tag{36}$$

with components:

$$\begin{aligned} v_{\rm a}(t) &= V_{\rm a}\sin(\omega_o t + \phi_{\rm a}(t))\,, \\ v_{\rm b}(t) &= V_{\rm b}\sin(\omega_o t + \phi_{\rm b}(t) - \zeta_{\rm b})\,, \\ v_{\rm c}(t) &= V_{\rm c}\sin(\omega_o t + \phi_{\rm c}(t) + \zeta_{\rm c})\,. \end{aligned} \tag{37}$$

Recall that the proposed approach operates in two dimensions, and that we use Clarke transform to convert (12) to the two-dimensional (α,β) plane.

1) Balanced Three-Phase Voltage: We discuss two examples: the first example involves a stationary condition, whereas the second example considers a signal with time-varying voltage magnitude. In both examples, the angular frequency is constant and equal to ω_o. The parameters used are:

- E1: $V_i = 12$ kV, with $\omega_o = 100\pi$ rad/s, $\phi_i = 0$ and $\zeta_{\rm b} = \zeta_{\rm c} = \frac{2\pi}{3}$ rad.
- E2: $V_i = 12{+}3\sin(\pi t)$ kV, with $\omega_o = 100\pi$ rad/s, $\phi_i = 0$ and $\zeta_{\rm b} = \zeta_{\rm c} = \frac{2\pi}{3}$ rad.

Figure 1 shows the phase voltages, the geometric frequencies ω_a and ω_κ, as well as the instantaneous frequency $\omega_{\rm PLL}$ obtained with a conventional SRF-PLL for E1 and E2. As expected, since the voltage is balanced and the curve in the plane (α,β) is a circle, there is a perfect match between the estimations obtained with the two differential geometry-based methods. Note, however, that the two approaches return the right results for two different reasons: the Frenet frame-based formula returns a constant ω_κ because the circle has a constant curvature; whereas the proposed affine differential geometry approach returns a constant ω_a because the circle is a special case of an ellipse. We note that the conventional PLL also works well in this balanced-voltage case.

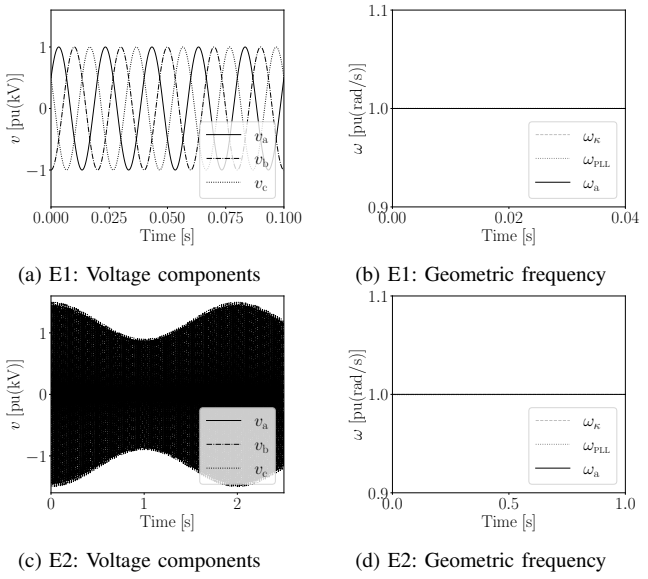

(a) E1: Voltage components (b) E1: Geometric frequency

(c) E2: Voltage components (d) E2: Geometric frequency

Fig. 1: Balanced three-phase voltages and estimated frequency.

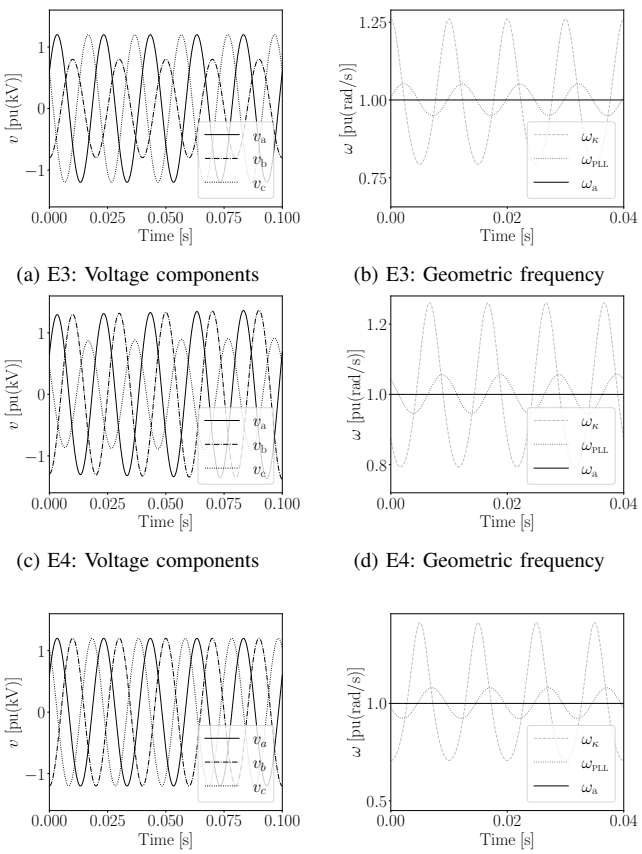

(a) E3: Voltage components (b) E3: Geometric frequency

(c) E4: Voltage components (d) E4: Geometric frequency

(e) E5: Voltage components (f) E5: Geometric frequency

Fig. 2: Unbalanced three-phase voltages and estimated frequencies.

2) Unbalanced Three-Phase Voltage: Three examples of unbalanced voltages with constant angular frequency ω_o are considered in this section. The first example involves unequal constant voltage magnitudes; the second example examines a system with unequal and time-varying voltage magnitudes; and the third example examines a system with unequal phase displacements. The following three cases are considered:

- E3: $V_{\text{a}} = V_{\text{c}} = 12$ kV, $V_{\text{b}} = 8$ kV, with $\omega_o = 100\pi$ rad/s, $\phi_i = 0$ and $\zeta_{\text{b}} = \zeta_{\text{c}} = \frac{2\pi}{3}$ rad.
- E4: $V_{\text{a}} = V_{\text{c}} = 12{+}3\sin(\pi t)$ kV, $V_{\text{b}} = 8{+}2\sin(2\pi t)$ kV, with $\omega_o = 100\pi$ rad/s, $\phi_i = 0$ and $\zeta_{\text{b}} = \zeta_{\text{c}} = \frac{2\pi}{3}$ rad.
- E5: $V_{\text{a}} = V_{\text{b}} = V_{\text{c}} = 12$ kV, with $\omega_o = 100\pi$ rad/s, $\phi_i = 0$ and $\zeta_{\text{b}} = \frac{-2\pi}{3}, \zeta_{\text{c}} = \frac{1.5\pi}{3}$ rad.

Figure 2 shows the voltage components and estimated geometric and PLL frequencies for examples E3-E5. In all these examples, the curves in the (α, β) plane are ellipses. This means that the curvature obtained using the Frenet frame is time-varying and periodic, thus leading to a time-varying and periodic ω_κ. Moreover, the conventional PLL also outputs a time-varying frequency in the form of a significant ripple around the frequency ω_o. On the other hand, the proposed affine geometry formula returns a constant ω_a equal to ω_o (in pu), which is consistent with the expected in this case result.

B. Three-Phase Voltage with Time-Varying Frequency

Two examples of three-phase system with varying angular frequency are considered in this section. The first example considers a voltage with angular frequency that varies periodically around its average value. This example is used to resemble the transient behavior of the voltage following a contingency in a power system, where voltage phase angle oscillations arising due to electro-mechanical swings of synchronous machines are poorly damped and thus sustain for a relatively long time. The second example is an extreme and uncommon situation in power systems, where the components of the three-phase voltage are time-varying and have unequal angular frequencies. The following parameters are used:

- E6: $V_i = 12$ kV, with $\omega_o = 100\pi$ rad/s and $\zeta_{\text{b}} = \zeta_{\text{c}} = \frac{2\pi}{3}$ rad and $\phi_i(t) = \pi\sin(0.4\pi t)$ rad.
- E7: $V_i = 12$ kV, with $\omega_o = 100\pi$ rad/s and $\zeta_{\text{b}} = \zeta_{rmc} = \frac{2\pi}{3}$ rad and $\phi_{\text{a}}(t) = \phi_{\text{b}}(t) = \pi\sin(0.4\pi t), \phi_{\text{c}}(t) = 1.1\pi\sin(0.4\pi t)$ rad.

Figure 3a shows the estimated frequency with the proposed formula, the frequency estimated with the PLL, and the geometrical frequency ω_κ, for E6. Despite the approximations imposed by assuming (24) and (25), we note that (26) is able to precisely track the exact instantaneous frequency. In this example, also ω_κ and ω_{PLL} track well IF. On the other hand, for E7, while ω_a and ω_{PLL} still track well the exact frequency, ω_κ shows significant fluctuations. This behavior is illustrated in Fig. 3b.

C. Stationary Three-Phase Voltage with Harmonics

As a last example on three-phase voltage, we discuss the effect of harmonics on the estimation of the frequency based on (26). A fundamental condition for the affine differential geometry approach to work properly is that (2) is satisfied at all times. Harmonics, however, introduce inflection points, that is, points for which $[\dot{\boldsymbol{x}}, \ddot{\boldsymbol{x}}] \leq 0$. Moreover, since the term $[\dot{\boldsymbol{x}}, \ddot{\boldsymbol{x}}]$

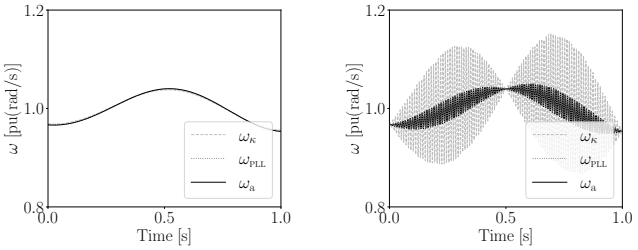

(a) E6 (b) E7

Fig. 3: Estimated angular frequency.

appears in the denominator of (26), this leads to numerical issues. Figure 4b shows the performance of (26) as well as of the PLL and Frenet-based estimated frequencies for a stationary balanced three-phase voltage. For the fundamental frequency, $V_i = 12$ kV, with $\omega_o = 100\pi$ rad/s and $\zeta_{\text{b}} = \zeta_{\text{c}} = \frac{2\pi}{3}$ rad and $\phi_i(t) = 0$ are assumed. Then, 7-th and 11-th harmonics are added with magnitudes $0.02V_i$ and $0.01V_i$, respectively. To overcome numerical issues, we have set $\omega_a = 0$ if $[\dot{\boldsymbol{x}}, \ddot{\boldsymbol{x}}] \leq 0$. As expected, in this scenario, ω_a shows a poor performance. The best estimation is obtained with the PLL.

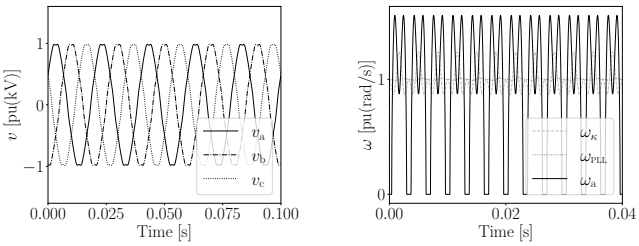

(a) Voltage components (b) Estimated angular frequency

Fig. 4: E8: Three-phase voltage with harmonics and estimated angular frequency.

D. IEEE 39-Bus System in Unbalanced Conditions

In this section, the accuracy of (26) is tested using a fully-fledged EMT model of the IEEE 39-bus system. The system setup is the same as the unbalanced scenario described in [24], where it was utilized to show the performance of the Frenet frame-based frequency estimation. In particular, the power consumption of all 19 loads of the system is unbalanced, with imbalances ranging from 5 to 10% on one of the phases. A three-phase fault is simulated at bus 4. The fault occurs at $t = 0.2$ s and is cleared at $t = 0.3$ s. The behavior of the three-phase voltage at bus 26 following the contingency is illustrated in Fig. 5.

Figure 6 shows the results of the frequency estimation for the unbalanced voltage at bus 26. The ω_a is more accurate than ω_{PLL}. Note that (26) has been evaluated using numerical differentiation of the time series of the three-phase voltage components that have a constant time sampling rate of 10 ms. The numerical derivatives are filtered using a second order Butterworth digital filter and a IIR filter. Note that, in this scenario, ω_κ shows a bigger ripple than ω_{PLL} and, thus ω_κ is omitted in Fig. 6 for clarity. The interested reader can find a comprehensive comparison between PLL frequency estimations and ω_κ in [24].

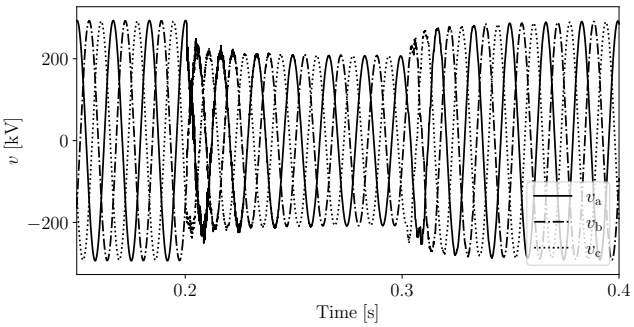

Fig. 5: Voltage at bus 26 of IEEE 39-bus system following a three-phase fault at bus 4.

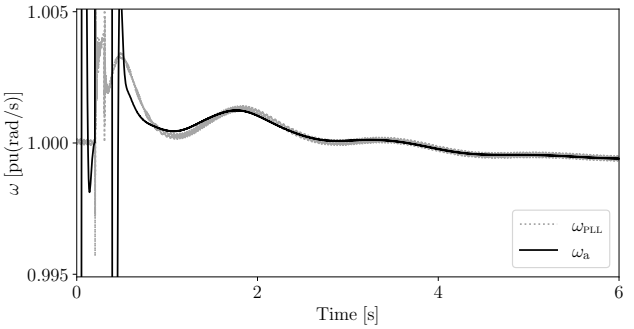

Fig. 6: Estimated frequency for IEEE 39-bus system for unbalanced time-varying voltage.

E. Single-Phase Voltage

This last example illustrates the performance of the proposed formula (26) when applied to a single-phase voltage with time-varying angular frequency $\omega t + \phi(t)$ and constant amplitude V:

$$v(t) = V \sin(\omega_o t + \phi(t)) \,. \tag{38}$$

The parameters considered for this example are: $V = 12$ kV, $\omega_o = 100\pi$ rad/s and $\phi(t) = 0.05\omega_o e^{-t}(1 - \cos(\pi t))$ rad.

As discussed in Section III-B, we construct the second dimension by using the derivative of the original signal, as in (27). Figure 7 illustrates the accuracy of (26) in matching the actual analytical value of the instantaneous frequency, that is, $\text{IF} = \omega_{\text{o}} + \dot{\phi}$.

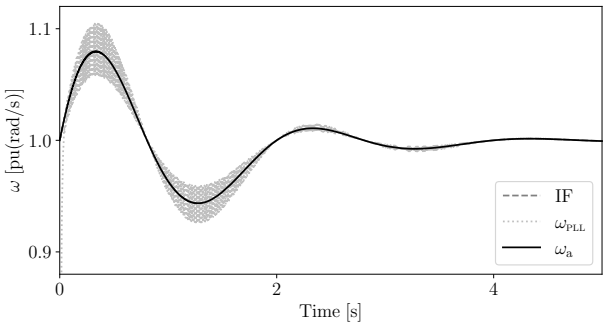

Fig. 7: Estimated frequency, analytical instantaneous frequency (IF) and frequency estimated using a phase shift for the single-phase voltage.

Figure 7 also shows the frequency estimated using a conventional PLL where the quadrature signal is obtained using $v(t-\tau)$, where the transport delay is $\tau = 0.25\,T = 0.5\,\pi/\omega_o$. Despite the approximations resulting from the assumptions (33) and (34), also in this case the proposed approach shows very good accuracy, whereas the PLL shows some ripples due to the fact that the quadrature signal is not exact because the frequency is time-varying.

V. Conclusions

This paper presents an approach based on affine differential geometry to estimate the angular frequency of unbalanced three-phase voltages as well as of single-phase voltages. The main contribution of this work is the approximated formula (26), that estimates the angular frequency of the voltage through measurements of the voltage, and calculation of the first and second derivatives of the voltage itself.

Approximations based on the nature of typical power system transients are assumed in order to achieve a compact explicit expression of the proposed angular frequency estimation formula. Then, a variety of examples are provided to demonstrate the adequateness of such approximations and the performance of the proposed formula. When compared to PLLs as well as to the Frenet frame-based estimation from [23], the proposed formula proves to be accurate and robust in balanced and unbalanced conditions, as well as for voltages of time-varying magnitude and frequency.

Future work will focus on testing the proposed formula with real-world measurements and on extending its formulation to process signals with harmonic contents as well as with multi-phase systems with a number of phases higher than three.

References

[1] B. Liu, F. Zhuo, Y. Zhu, H. Yi, and F. Wang, "A three-phase PLL algorithm based on signal reforming under distorted grid conditions," *IEEE Transactions on Power Electronics*, vol. 30, no. 9, pp. 5272–5283, 2014.

[2] M. Eskandari and A. V. Savkin, "Robust PLL synchronization unit for grid-feeding converters in micro/weak grids," *IEEE Transactions on Industrial Informatics*, vol. 19, no. 4, pp. 5400–5411, 2022.

[3] P. Romano, M. Paolone, J. Arnold, and R. Piacentini, "An interpolated-DFT synchrophasor estimation algorithm and its implementation in an FPGA-based PMU prototype," in *IEEE PES General Meeting*. IEEE, 2013, pp. 1–6.

[4] J. Song, A. Mingotti, J. Zhang, L. Peretto, and H. Wen, "Fast iterative-interpolated dft phasor estimator considering out-of-band interference," *IEEE Transactions on Instrumentation and Measurement*, vol. 71, pp. 1–14, 2022.

[5] S. Reza, M. Ciobotaru, and V. G. Agelidis, "Accurate estimation of single-phase grid voltage fundamental amplitude and frequency by using a frequency adaptive linear Kalman filter," *IEEE Journal of Emerging and Selected Topics in Power Electronics*, vol. 4, no. 4, pp. 1226–1235, 2016.

[6] X. Nie, "Detection of grid voltage fundamental and harmonic components using Kalman filter based on dynamic tracking model," *IEEE Transactions on Industrial Electronics*, vol. 67, no. 2, pp. 1191–1200, 2019.

[7] S. Giarnetti, F. Leccese, and M. Caciotta, "Non recursive multi-harmonic least squares fitting for grid frequency estimation," *Measurement*, vol. 66, pp. 229–237, 2015.

[8] A. Pradhan, A. Routray, and A. Basak, "Power system frequency estimation using least mean square technique," *IEEE Transactions on Power Delivery*, vol. 20, no. 3, pp. 1812–1816, 2005.

[9] F. Wilches-Bernal, J. Wold, and W. H. Balliet, "A method for correcting frequency estimates for synthetic inertia control," *IEEE Access*, vol. 8, pp. 229 141–229 151, 2020.

[10] M. Mojiri, M. Karimi-Ghartemani, and A. Bakhshai, "Estimation of power system frequency using an adaptive notch filter," *IEEE Transactions on Instrumentation and Measurement*, vol. 56, no. 6, pp. 2470–2477, 2007.

[11] L. Hadjidemetriou, Y. Yang, E. Kyriakides, and F. Blaabjerg, "A synchronization scheme for single-phase grid-tied inverters under harmonic distortion and grid disturbances," *IEEE Transactions on Power Electronics*, vol. 32, no. 4, pp. 2784–2793, 2016.

[12] R. M. Santos Filho, P. F. Seixas, P. C. Cortizo, L. A. Torres, and A. F. Souza, "Comparison of three single-phase PLL algorithms for ups applications," *IEEE Transactions on Industrial Electronics*, vol. 55, no. 8, pp. 2923–2932, 2008.

[13] P. Hao, W. Zanji, and C. Jianye, "A measuring method of the single-phase ac frequency, phase, and reactive power based on the hilbert filtering," *IEEE Transactions on Instrumentation and Measurement*, vol. 56, no. 3, pp. 918–923, 2007.

[14] A. Sahoo, J. Ravishankar, and C. Jones, "Phase-locked loop independent second-order generalized integrator for single-phase grid synchronization," *IEEE Transactions on Instrumentation and Measurement*, vol. 70, pp. 1–9, 2021.

[15] M. S. Reza, F. Sadeque, M. M. Hossain, A. M. Ghias, and V. G. Agelidis, "Three-phase PLL for grid-connected power converters under both amplitude and phase unbalanced conditions," *IEEE Transactions on Industrial Electronics*, vol. 66, no. 11, pp. 8881–8891, 2019.

[16] H. Karimi, M. Karimi-Ghartemani, and M. R. Iravani, "Estimation of frequency and its rate of change for applications in power systems," *IEEE Transactions on Power Delivery*, vol. 19, no. 2, pp. 472–480, 2004.

[17] M. E. Meral, "Improved phase-locked loop for robust and fast tracking of three phases under unbalanced electric grid conditions," *IET Generation, Transmission & Distribution*, vol. 6, no. 2, pp. 152–160, 2012.

[18] A. Kulkarni and V. John, "Design of synchronous reference frame phase-locked loop with the presence of dc offsets in the input voltage," *IET Power Electronics*, vol. 8, no. 12, pp. 2435–2443, 2015.

[19] S. Golestan, M. Monfared, and F. D. Freijedo, "Design-oriented study of advanced synchronous reference frame phase-locked loops," *IEEE Transactions on Power Electronics*, vol. 28, no. 2, pp. 765–778, 2012.

[20] G. Escobar, C. N. M. Ho, S. Pettersson, M. J. Lopez-Sanchez, and A. A. Valdez-Fernandez, "Cascade three-phase PLL for unbalance and harmonic distortion operation (CSRF-PLL)," in *IECON*. IEEE, 2014, pp. 5489–5493.

[21] P. Rodríguez, J. Pou, J. Bergas, J. I. Candela, R. P. Burgos, and D. Boroyevich, "Decoupled double synchronous reference frame PLL for power converters control," *IEEE Transactions on Power Electronics*, vol. 22, no. 2, pp. 584–592, 2007.

[22] P. Rodríguez, A. Luna, I. Candela, R. Mujal, R. Teodorescu, and F. Blaabjerg, "Multiresonant frequency-locked loop for grid synchronization of power converters under distorted grid conditions," *IEEE Transactions on Industrial Electronics*, vol. 58, no. 1, pp. 127–138, 2010.

[23] F. Milano, G. Tzounas, I. Dassios, and T. Kerci, "Applications of the Frenet frame to electric circuits," *IEEE Transactions on Circuits and Systems I: Regular Papers*, vol. 69, no. 4, pp. 1668–1680, 2021.

[24] F. Milano, G. Tzounas, I. Dassios, M. A. A. Murad, and T. Kërçi, "Using differential geometry to revisit the paradoxes of the instantaneous frequency," *IEEE Open Access Journal of Power and Energy*, 2022.

[25] F. Milano, "A geometrical interpretation of frequency," *IEEE Transactions on Power Systems*, vol. 37, no. 1, pp. 816–819, 2021.

[26] F. Milano, "The Frenet frame as a generalization of the Park transform," *IEEE Transactions on Circuits and Systems I: Regular Papers*, vol. 70, no. 2, pp. 966–976, 2022.

[27] A. D. Lewis, "The bountiful intersection of differential geometry, mechanics, and control theory," *Annual Review of Control, Robotics, and Autonomous Systems*, vol. 1, pp. 135–158, 2018.

[28] M. Craizer, T. Lewiner, and J.-M. Morvan, "Parabolic polygons and discrete affine geometry," in *Brazilian Symposium on Computer Graphics and Image Processing*. IEEE, 2006, pp. 19–26.

[29] T. Flash and A. A. Handzel, "Affine differential geometry analysis of human arm movements," *Biological Cybernetics*, vol. 96, pp. 577–601, 2007.

[30] K. Nomizu and T. Sasaki, *Affine differential geometry: geometry of affine immersions*. Cambridge University Press, 1994.

[31] E. Calabi, P. J. Olver, and A. Tannenbaum, "Affine geometry, curve flows, and invariant numerical approximations," *Advances in Mathematics*, vol. 124, no. 1, pp. 154–196, 1996.

Ali Alshawabkeh received the B.Sc. in Energy Engineering and Electric Power from German Jordanian University in 2017 and the M.Sc. in Power and Data Engineering from Offenburg University, Germany, in 2021. In 2022, he joined the PhD program in Electrical Power Engineering of University College Dublin, Ireland. He is funded by Sustainable Energy Authority of Ireland (SEAI) under project FRESLIPS, Grant No. RDD/00681.

Georgios Tzounas (M'21) received the Diploma (M.E.) in Electrical and Computer Engineering from the National Technical Univ. of Athens, Greece, in 2017, and the Ph.D. from University College Dublin (UCD), Ireland, in 2021. In Jan.-Apr. 2020, he was a visiting researcher at Northeastern Univ., Boston, MA. From Oct. 2020 to Apr. 2023, he was a postdoctoral researcher with UCD (2020-2022) and ETH Zürich (2022-2023). Since Apr. 2023, he has been an Assistant Professor with the School of Electrical and Electronic Engineering at UCD. His research interests include stability analysis and control of power systems.

Federico Milano (F'16) received from the University of Genoa, Italy, the ME and Ph.D. in Electrical Engineering in 1999 and 2003, respectively. In 2013, he joined University College Dublin, Ireland, where he is a full professor. He is an IEEE Distinguished Lecturer, a senior editor of the IEEE Transactions on Power Systems, an IET Fellow, and an editor in chief of the IET Generation, Transmission & Distribution. He is chair of the IEEE Power System Stability Controls Subcommittee; chair of the Technical Program Committee of PSCC 2024; and a member of the Cigre Irish National Committee. His research interests include power system modeling, control and stability analysis.